

Oxygen vacancy clusters on ceria: Decisive role of cerium *f* electrons

Changjun Zhang,¹ Angelos Michaelides,² David A. King,¹ and Stephen J. Jenkins^{1,*}

¹*Department of Chemistry, University of Cambridge, Lensfield Road, Cambridge CB2 1EW, United Kingdom*

²*Department of Chemistry, Materials Simulation Laboratory, and London Centre for Nanotechnology, University College London, London WC1H 0AH, United Kingdom*

(Received 27 November 2008; published 20 February 2009)

Defects such as oxygen vacancies dominate the electronic and chemical properties of ceria. However, fundamental understanding of such defects, especially clusters of vacancies, is sparse. In this work, we use density-functional theory with the addition of the Hubbard U term to investigate various oxygen vacancies, including the vacancy monomer, dimer, trimer, and tetramer, in which subsurface vacancies can also be involved. We show that the individual surface and subsurface vacancies have very similar stabilities; the vacancy dimer consisting of two surface vacancies, which is not reported experimentally, is stable in theory; between the two vacancy trimers observed in experiments, the triangular surface vacancy cluster is more stable than the double linear surface vacancy cluster containing a subsurface vacancy, which agrees with some experiments but disagrees with some others; and the linear vacancy tetramer emerges as the most stable among the possible tetramers containing subsurface vacancies, although it is less stable than those containing no subsurface vacancies. These findings are rationalized in terms of the electronic change upon the removal of oxygen, namely, the localization of resulting excess electrons on Ce f orbitals. We identify a correlation between the energy levels of the occupied f states of reduced Ce ions and their coordination numbers, which proves pivotal in interpreting formation energy and stability of various vacancies. Comparisons are made with experiments and apparent discrepancies are discussed. Results for gold adsorption on the vacancy clusters are presented, and the implications these have in catalysis are briefly discussed.

DOI: [10.1103/PhysRevB.79.075433](https://doi.org/10.1103/PhysRevB.79.075433)

PACS number(s): 73.20.At, 61.72.jd, 71.15.Nc, 71.15.Mb

I. INTRODUCTION

The rare-earth oxide ceria (CeO_2) has recently emerged as one of the most interesting oxides both technologically and scientifically. Materials based on CeO_2 are finding novel use in a variety of processes such as automotive exhaust catalysis, water-gas shift (WGS) reactions, fuel cells, and production and purification of hydrogen.^{1,2} These applications of CeO_2 are largely attributed to its remarkable oxygen-storage capability, i.e., the ability to undergo rapid redox cycles by releasing and storing oxygen.³ Consequently, oxygen vacancy defects can play a central role: surface lattice oxygen may act as an oxidant for adsorbates, thus creating oxygen vacancies (i.e., Mars–van Krevelen mechanism⁴); and vacancies may serve as binding sites for catalytically active species, thus promoting activity of the catalyst (e.g., in the WGS reaction catalyzed by Au/CeO_2).^{5,6} To elucidate the roles of ceria played in those applications, it is therefore of great importance to understand the nature of oxygen vacancies.

With scanning tunneling microscopy (STM) and dynamic force microscopy (DFM), structures of O vacancies at the reduced $\text{CeO}_2\{111\}$ surfaces have been investigated.^{7–12} In the first atomically resolved images produced by Nörenberg and Briggs,⁷ oxygen vacancy clusters (denoted as VCs hereafter) were observed at the topmost layer of the surface, and the dominant type of VC was of triangular shape containing three O vacancies, schematically shown in Fig. 1. In contrast, Namai *et al.*⁹ suggested that linear alignments of O vacancies, consisting of two or more vacancies, are the major multiple defects, which appear in three different orientations reflecting the threefold symmetry of the $\{111\}$ surface. The discrepancy between these experiments was attributed to

“different sample treatments.”⁹ More detailed structures of O vacancies were recently shown by Esch *et al.*¹¹ With STM and STM simulations, they found that for the slightly reduced $\text{CeO}_2\{111\}$ surface, both SV and SSV were present with similar concentrations. Upon prolonged annealing, VCs appeared, with linear surface vacancy clusters (LSVCs) being the most dominant and triangular SVTs being the next most abundant. The authors also proposed that VCs with more than two vacancies exclusively expose reduced Ce ions (Fig. 1), and that to satisfy this interesting trend, each LSVC must incorporate a subsurface oxygen vacancy. In a more recent DFM study by Torbrügge *et al.*,¹² explicit evidence of isolated SSV buried at the third layer of the $\text{CeO}_2\{111\}$ surface was found. Furthermore, SSVs themselves exhibited interesting structures: at high concentrations, SSVs appear in ordered arrays with a tendency to form linear patterns, leaving defect-free spacing of two lattice constants in between.

The discovery of VCs in ceria is of great significance. As pointed out by Campbell and Peden,¹³ the groups of exposed Ce^{3+} ions in the VCs would become a potentially potent surface site for catalysis, as adsorbed gases or reaction intermediates could interact simultaneously with several Ce^{3+} ions. Such VCs may even direct adsorbed metal nanoparticles into specific shapes that may have advantages in catalysis. However, images of VCs, particularly the *shapes* of VCs, are not consistent in previous studies.^{7,9,11} There is also a notable lack of theoretical understanding of VCs in ceria, and most studies have so far concentrated on an isolated vacancy.^{14–16} In the present work, we have therefore undertaken a detailed theoretical investigation on a series of oxygen vacancies on $\text{CeO}_2\{111\}$, including vacancy monomer, dimer, trimer, and tetramer. We focus here on two fundamental aspects: (i) the energy required to form the oxygen defects

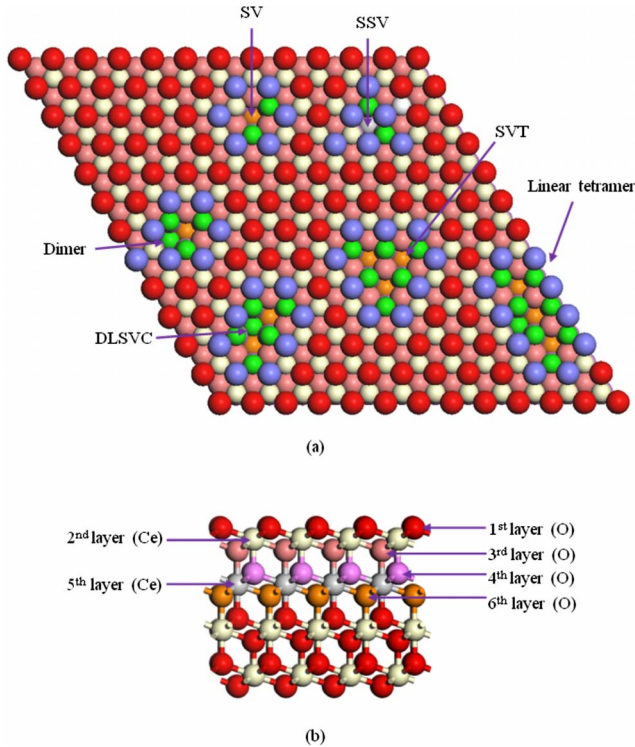


FIG. 1. (Color online) (a) Examples of a surface vacancy (SV), a subsurface vacancy (SSV), a vacancy dimer, a triangular surface vacancy trimer (SVT), a double linear surface vacancy cluster (DLSVC), and a linear vacancy tetramer at the $\text{CeO}_2\{111\}$ surface. We adopt the same abbreviations as used in Ref. 11. The reduced Ce ions and the O ions around them are highlighted in green and blue, respectively, in the online version of this article; in black and white print, those refer to the Ce ions exposed to the vacancies and the rim O atoms around the vacancies, respectively. Note that the spin arrangement for the dimer proposed in Ref. 11 is likely to be incorrect, as discussed in Sec. IV B. (b) The color coding for atoms at different layers is depicted.

and (ii) the electronic structure of the reduced systems, as highlighted in a recent review paper on O vacancies in transition-metal and rare-earth oxides.¹⁷ In particular, owing to the strong $f(\text{Ce})$ electron localization effect, reduction of the ceria surface leads to a change of valence from Ce^{4+} to Ce^{3+} , which differs from situations on many other oxide surfaces where either F center or electron delocalization would occur upon reduction.¹⁷ This rather unique electron localization feature therefore holds the key to understanding the intriguing nature of the vacancies on ceria and their implications in catalysis.

The present paper is organized as follows. Calculation details are given in Sec. II. In Sec. III, we introduce all types of vacancies considered and report vacancy formation energies. Following that, we discuss electronic structures and illustrate the physical origin of the relative stabilities of those vacancies in Sec. IV. In Sec. V, we make comparisons with available experimental data and discuss the discrepancies that have been found. In Sec. VI, we present some results of Au adsorption on VCs which are likely to be relevant to and have implications for catalysis. Our conclusions are summarized in Sec. VII.

II. METHODOLOGY

We carry out spin-polarized calculations within the density-functional theory (DFT) framework, as implemented in the Vienna *Ab initio* Simulation Program (VASP), a plane-wave pseudopotential DFT package.^{18–20} We use the projector-augmented wave method to describe the effect of the core electrons on the valence electrons in the system.^{21,22} The Ce $5s$, $5p$, $5d$, $4f$, and $6s$ electrons; the O $2s$ and $2p$ electrons; and the Au $5d$, $6s$, and $6p$ electrons are treated as valence electrons. For the electron exchange-correlation functional the generalized gradient approximation (GGA) of Perdew²³ and Wang is used.

We choose the DFT+ U methodology,^{24,25} which has proven to be essential in descriptions of reduced ceria systems.¹⁷ In this approach, the Hubbard parameter U is introduced to account for the strong on-site Coulomb repulsion among the localized Ce $4f$ electrons. In practice, however, the choice of this parameter is often empirical, which is to say that the U value is adjusted to reproduce properties known from experiments. There are a host of papers devoted to the discussion of appropriate U values.^{14,15,26–30} In studying reduced ceria, Nolan *et al.*¹⁴ suggested $U=5.0$ eV for GGA+ U , as for $U<5.0$ eV significant delocalization still persists. Fabris *et al.*¹⁵ derived $U=5.3$ eV for local-density approximation (LDA) and $U=4.5$ eV for GGA+ U when using the maximally localized Wannier orbital as the projector function. Andersson *et al.*²⁹ showed that $U\approx 6.0$ eV for LDA+ U and $U\approx 5.0$ eV for GGA+ U provide a consistent description of pure CeO_2 and Ce_2O_3 plus vacancies in CeO_2 . Castleton *et al.*³⁰ also suggested that the best overall choice is $U\approx 6.0$ eV for LDA+ U and $U\approx 5.5$ eV for GGA+ U . We note that although suggestions of U values vary, the optimal ones appear to be around 5.0 eV for GGA+ U and 6.0 eV for LDA+ U . We therefore use GGA+ U ($U=5.0$ eV) in the current work. We also carry out tests with GGA+ U ($U=4.5$ or 5.5 eV) and LDA+ U ($U=6.0$ eV), and our conclusions are not qualitatively affected by these choices.

The $\{111\}$ face of ceria features termination of stoichiometric O-Ce-O trilayers stacked along the $[111]$ direction (Fig. 1), and is the thermodynamically most stable facet. In order to accommodate VCs as well as to minimize the interaction between VCs, a large (4×4) unit cell is chosen. In some cases (e.g., vacancy tetramers), tests with an even larger (4×6) cell are performed, and no significant difference is found: the formation energy of vacancy tetramers differs by only 0.03 eV from the calculations in the two cells. The slabs employed in our calculations have nine atomic layers, which is a common choice in studying ceria surfaces.^{14–16} The vacuum regions for the slabs are generally around 12 Å. During structure optimizations atoms are allowed to relax until the forces are smaller than 0.03 eV/Å, except those in the lowest three layers that are constrained to the equilibrium positions calculated for the defect-free supercell. We note that in the cases involving subsurface O vacancies and the reduction of inner Ce ions, further relaxation of the inner atoms might be necessary. Therefore, calculations are also performed with slabs containing 12 atomic layers (including up to 192 atoms) for vacancy dimers and trimers. However, we find that characteristic electronic features, va-

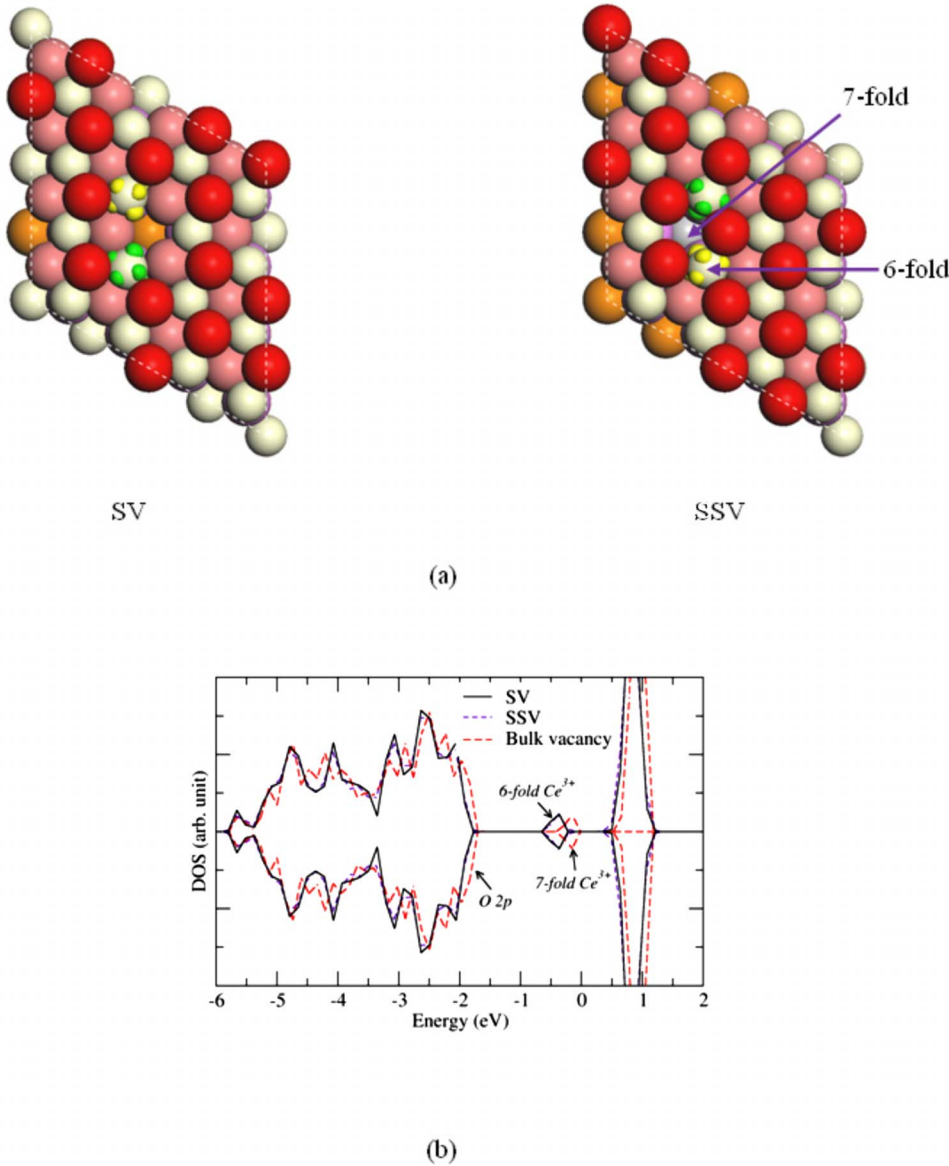


FIG. 2. (Color online) (a) The electron densities of the gap states (green and yellow areas in the online version of this article or the dark areas around Ce atoms in the black and white print), which are localized on the two Ce ions neighboring the SV and SSV. The color coding of the atoms is the same as in Fig. 1. Two different Ce neighbors for SSV are indicated. (b) The spin-resolved total density of states (DOS), which are calculated with a smearing width of 0.04 eV. The Fermi levels of each system are set to zero. For comparison, the DOS of the surface with a bulk vacancy, defined in the text, is also included. For best viewing, the DOS corresponding to the f states at the band gaps is multiplied by a factor of 5 in order to allow the features to be more clearly seen.

cancy formation energies, and relative stabilities are very similar between calculations from the 9-layer and the 12-layer slabs. To reduce the computational cost, we therefore use the 9-layer slab for the calculations of vacancy tetramers. The sampling of the Brillouin zone was performed with a $2 \times 2 \times 1$ Monkhorst-Pack k -point mesh. The number of plane waves, used to expand the Kohn-Sham orbitals, is controlled by a cutoff energy of 400 eV, which is sufficient to obtain well-converged results.³¹

It is well known that upon creation of an O vacancy, the two excess electrons left behind by the removed O would localize on the two neighboring Ce ions, leading to the reduction of Ce⁴⁺ to Ce³⁺.¹⁷ As will be shown shortly, the location of the Ce³⁺ ions is vital in interpreting the stability of reduced surfaces. Thus, for each vacancy (or VC), we have examined different starting spin configurations (i.e., different locations of Ce³⁺), in order to identify the most stable configuration. We find that the energy differences between different spin configurations obtained for each vacancy (or VC) are almost negligible. For example, for the surface with

SV, both ferromagnetic and antiferromagnetic ground states are found,^{15,32} but the antiferromagnetic arrangement is only 0.02 eV more stable. For the surface with SSV, the antiferromagnetic state is marginally more stable by 0.01 eV than the ferromagnetic one. Therefore, we report below only the most stable configurations, without overinterpreting the alignment of neighboring spins.

III. VARIOUS VACANCIES AND VACANCY FORMATION ENERGIES

We first consider single-oxygen vacancies by removing either a topmost surface O atom or a subsurface O atom at the third layer from the stoichiometric surface, as shown in Fig. 2. Also shown are electron densities of the spin states (i.e., the occupied f states of Ce³⁺ ions), which will be detailed in Sec. IV. To illustrate stability of these vacancies, we list in Table I the formation energy per vacancy (ΔE_v^d),

TABLE I. The averaged vacancy formation energy (ΔE_v^a) and the formation energy of the n th vacancy (ΔE_v^n in parentheses). Both energies (in eV) are defined in the text. As also stated in the text, ΔE_v^4 for tetramers I–III are calculated with respect to trimer DLSVC and those for tetramers IV and V are calculated with respect to trimer SVT. The structures of VCs are shown in Figs. 2–6.

	ΔE_v^a (ΔE_v^1)	ΔE_v^a (ΔE_v^2)	ΔE_v^a (ΔE_v^3)	ΔE_v^a (ΔE_v^4)
Monomer SV	2.23 (2.23)			
Monomer SSV	2.17 (2.17)			
Dimer I		2.35 (2.53)		
Dimer II		2.38 (2.58)		
Trimer SVT			2.25 (2.30)	
Trimer DLSVC			2.58 (3.27)	
Tetramer I				2.59 (2.34)
Tetramer II				2.69 (2.71)
Tetramer III				2.72 (2.82)
Tetramer IV				2.35 (2.33)
Tetramer V				2.34 (2.32)

$$\Delta E_v^a = \left(E_{\text{slab}}^n - E_{\text{slab}}^{\text{stoi}} + \frac{n}{2} E_{\text{O}_2} \right) / n, \quad (1)$$

where E_{slab}^n , $E_{\text{slab}}^{\text{stoi}}$, and E_{O_2} are energies of a surface with n O vacancies, the perfect stoichiometric surface, and an O_2 molecule, respectively. As can be seen, the two reduced surfaces have similar energies: the surface with SSV is slightly more stable (by 0.06 eV) than that with SV. We note that previous GGA+ U calculation also slightly preferred SSV to SV by 0.26 or 0.14 eV, but previous LDA+ U calculation predicted SV to be more stable by 0.03 or 0.15 eV, when using the atomic orbitals or the localized Wannier orbitals as the projector functions, respectively, in the expression of the U term.¹⁵ Although the relative stability of these defects appears to depend on the methodology, we consider that the energy differences are insignificant since the vacancy formation energy is large (~ 2.2 eV in Table I). Moreover, the similar energies of the two defects calculated in the present work agree with the experiment finding that SVs and SSVs have similar concentrations on the slightly reduced surfaces.¹¹

There are in principle two possible dimer vacancies (Fig. 3), which could consist of either one SV plus one SSV (dimer I) or two SVs (dimer II), although Esch *et al.*¹¹ claimed dimer I to be the only vacancy dimer that has been observed. Our calculations find that both dimers I and II are stable, with the former being 0.05 eV lower in energy than the latter, as can be seen from Table I. In addition to ΔE_v^a , we also list in Table I the energy for the n th vacancy formation (ΔE_v^n), given by

$$\Delta E_v^n = E_{\text{slab}}^n - E_{\text{slab}}^{n-1} + \frac{1}{2} E_{\text{O}_2}, \quad (2)$$

where E_{slab}^n and E_{slab}^{n-1} are the energies of surfaces with n and $n-1$ O vacancies. With respect to the most stable single vacancy (i.e., SSV), we calculate the formation energies for the

second vacancy (ΔE_v^2) to be 2.53 and 2.58 eV for dimers I and II, respectively, which are somewhat higher than ΔE_v^1 .

Moving to the vacancy trimer, we investigate the triangular SVT and the DLSVC,^{7–11} both of which were observed in experiments, although conclusions vary as to which of these is dominant. As shown in Fig. 4, SVT contains three surface vacancies, whereas DLSVC contains two surface vacancies and one subsurface vacancy. A common feature of the two VCs is that both are exposed to six Ce neighbors, which are just enough to accommodate the six excess electrons left behind by the three released O atoms. Our calculations show that SVT is 0.97 eV more stable than DLSVC: with respect to the most stable dimer (i.e., dimer I), the energies in forming the third O vacancy in SVT and DLSVC are 2.30 and 3.28 eV, respectively. This result agrees with the experiment of Nörenberg and Briggs,⁷ who stated that the defects first appear as triangular ones and form linear defects only at higher temperatures, but disagree with experiments of Namai *et al.*⁹ and Esch *et al.*,¹¹ who stated that the linear defects are the main type.

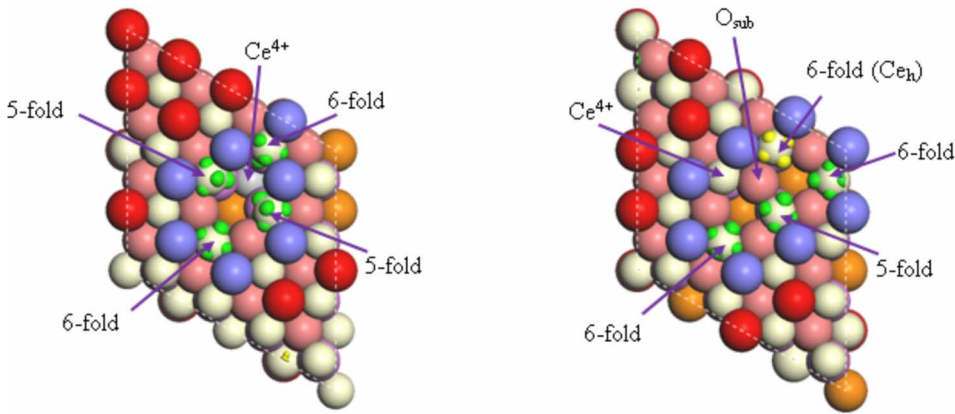
The vacancy tetramers are created by removing a further O atom from either DLSVC or SVT. Starting from DLSVC, we can create three distinct yet stable vacancy tetramers by removing one of the following O atoms, i.e., O_I , O_{II} , and O_{III} (Fig. 4), which are neighboring a *sixfold*, a *fivefold*, and a *fourfold* Ce^{3+} ion, respectively.³³ The resultant tetramers are denoted as tetramers I, II, and III in Fig. 5. Starting from trimer SVT, we can create two more tetramers by removing a surface O neighboring a fivefold Ce^{3+} or a surface O neighboring a sixfold Ce^{3+} , which are denoted as tetramers IV and V, respectively, in Fig. 6. In each of tetramers I–V, the two excess electrons left behind by the newly released O would find two adjacent Ce ions, so the trend that the VCs exclusively expose Ce^{3+} ions is preserved.

From values of ΔE_v^a in Table I, tetramers IV and V are clearly more stable (by at least 0.9 eV) than tetramers I–III, i.e., analogous to the relative stability between trimer SVT and DLSVC. With respect to the most stable trimer (i.e., SVT), the formation energies of the fourth O vacancy (ΔE_v^4) in tetramers IV and V are ~ 2.3 eV, which is close to ΔE_v^3 for trimer SVT or ΔE_v^1 for monomers. The values of ΔE_v^a in tetramers I–III would obviously be much higher if the same reference were used. Instead, we calculate ΔE_v^a in tetramers I–III with respect to DLSVC, and summarize them in Table I. Interestingly, the value of this redefined ΔE_v^a for tetramer I, which has a linear shape, is also close to ΔE_v^3 for trimer SVT or ΔE_v^1 for monomers. The implications of this result will be discussed in Sec. V.

IV. ELECTRONIC STRUCTURE

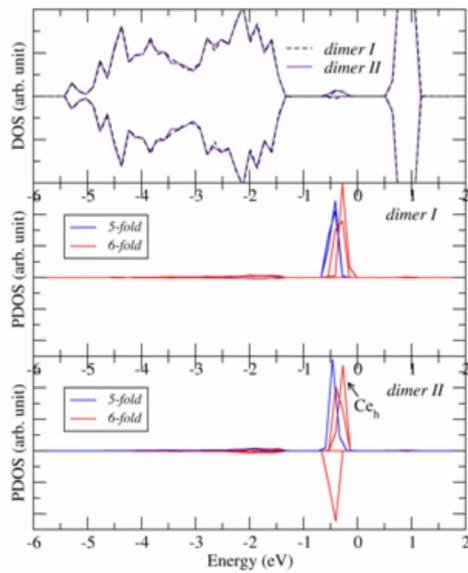
A. Vacancy monomer

The similar stabilities of SV and SSV can be ascribed to their similar electronic structures. Figure 2 shows the DOSs for the two surfaces (the solid and the short-dashed curves in the bottom panel of Fig. 2). In both cases, the DOS features an occupied band near the Fermi level (E_F), which is the so-called gap state derived from the reduction of Ce^{4+} to Ce^{3+} . From the electron-density plots of the gap states (the



dimer I dimer II

(a)



(b)

FIG. 3. (Color online) (a) The electron densities of the gap states, which are localized on the four Ce ions neighboring the vacancy dimers (I and II). The coordination of each reduced Ce ion is shown. (b) The total DOSs and the Ce $4f$ partial densities of states (PDOSs) for the surfaces containing these dimers, the latter of which are rescaled so that the features can be seen more clearly.

top parts of Fig. 2), regardless of whether the O vacancy is SV or SSV, the two excess electrons localize on the same two second-layer Ce ions. Hence, the DOSs of the two surfaces become almost indistinguishable, which has also been shown in a previous study.¹⁵

A question may arise in the case of SSV: why do the excess electrons populate the Ce ions at the outer second layer rather than that at the inner fifth layer (indicated in Fig. 2) which also neighbors SSV? We consider that the answer to the question lies in a simple fact: the fifth-layer Ce is *sevenfold* and the second-layer Ce is *sixfold*. Because the sevenfold Ce has more O neighbors, its reduction (i.e., receiving electrons) would induce a larger electrostatic repulsion with its O neighbors and consequently weaken the ionic bonding between them to a larger extent than the reduction of the sixfold Ce would do. To demonstrate this idea, we create an O vacancy at the fifth layer (i.e., a vacancy that might be considered as lying in the bulk), where the Ce ions neighboring the vacancy, all being sevenfold, would have to

accommodate the excess electrons left behind by the released O atom. As can be seen from the DOS (the long-dashed red curve), the energies of the occupied f states of the sevenfold Ce^{3+} are indeed higher than those of the sixfold one. Moreover, the O $2p$ states also appear at higher energies than those for SV or SSV, clearly indicating the more weakened ionic bonding between O and Ce for the surface with the bulk vacancy. Hence, it is not surprising that the surface with the “bulk” vacancy is much less stable (by 1.51 eV) than that with SV or SSV.

B. Vacancy dimer

We first comment on an electronic model proposed previously for dimer I (shown in Fig. 1),¹¹ in which the four excess electrons reduce four Ce^{4+} to Ce^{3+} (highlighted in green for a dimer). We note that this model includes an inner Ce^{3+} at the fifth layer, whereas an outer Ce ion at the second layer (neighboring the defect, and available to accept elec-

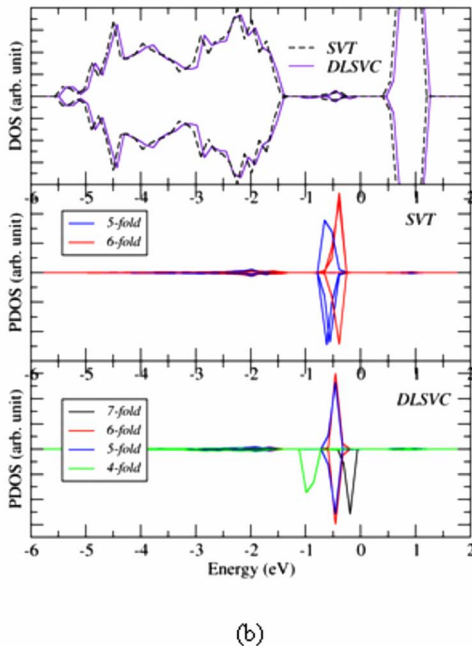
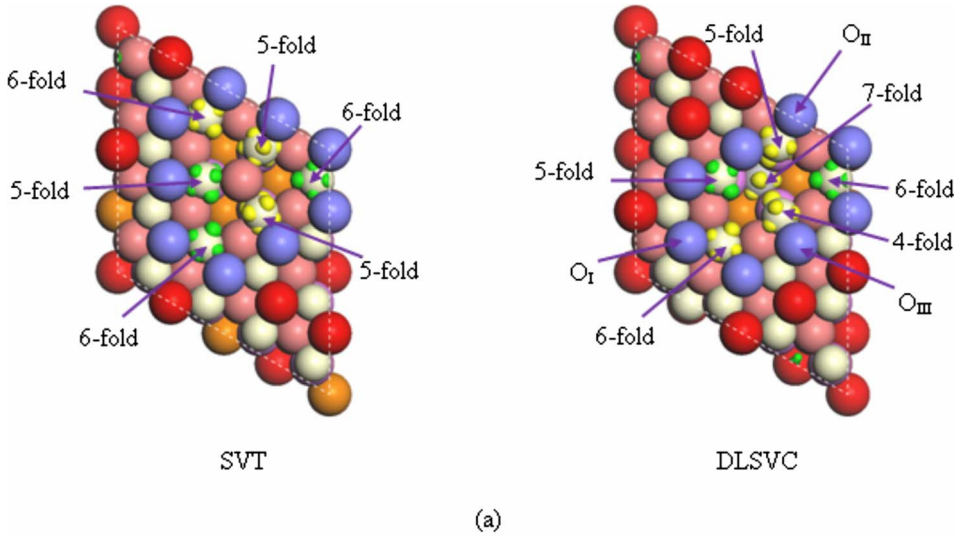


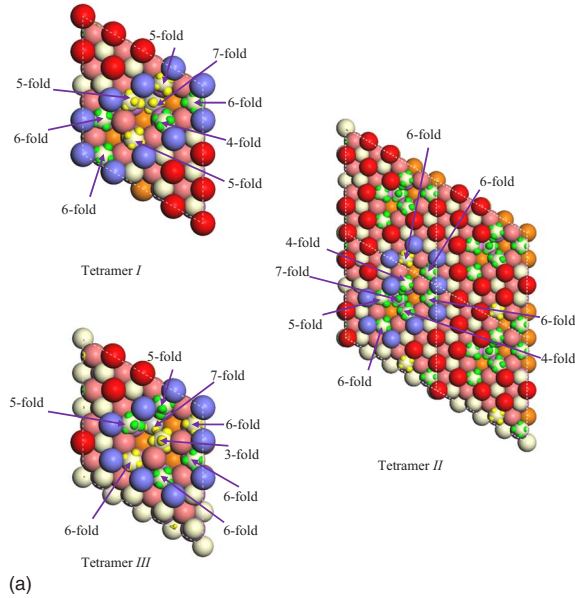
FIG. 4. (Color online) (a) The electron densities of the gap states, which are localized on the six Ce ions neighboring the vacancy trimers (SVT and DLSVC). (b) The total DOS and the Ce 4*f* partial DOS for the surfaces containing these tetramers.

trons) remains Ce⁴⁺, and that no calculation detail was given for the dimer. This electronic arrangement is surprising because, as we showed in Sec. IV A, electrons would tend to populate the lesser coordinated outer Ce ion. Indeed, such an electronic structure has not been found in our study: even if we started a calculation with the initial spins being assigned exactly the same as proposed previously, the spin on the fifth-layer Ce would relocate onto the second-layer Ce. In the stable structure of dimer I, all four Ce³⁺ ions locate at the second layer, as illustrated in Fig. 3.

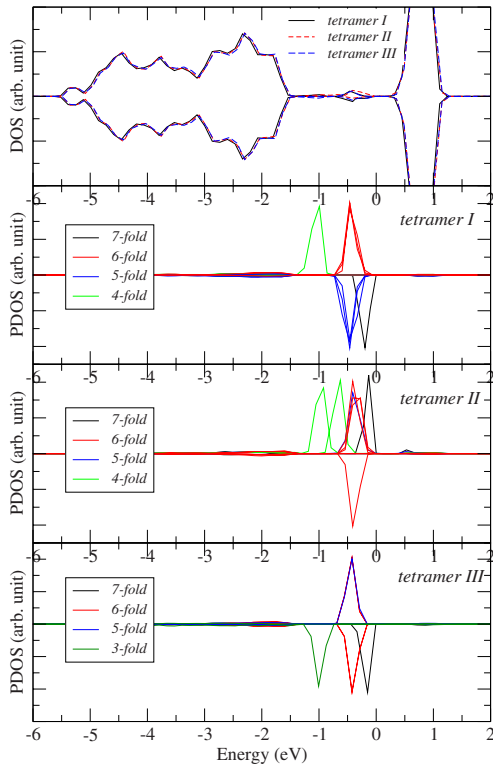
It is interesting to note that the four Ce³⁺ ions for dimer I include two fivefold and two sixfold ones. Therefore, we also plot in Fig. 3 the PDOS for the 4*f* states of the four ions, in addition to the total DOS. The PDOS reveals that the occupied *f* states of the two fivefold Ce³⁺ (the blue curves) are lower in energy than those of the two sixfold Ce³⁺ (the red curves). This feature, along with the relative energy levels of

the occupied *f* states of the sevenfold and sixfold Ce³⁺ observed in Sec. IV A, suggests a correlation between the coordination numbers of Ce³⁺ ions (n^{Ce}) and the energies of their occupied *f* states (e^f): the larger n^{Ce} is, the higher e^f would be. Another point worthy of noting is the splitting of e^f for the two sixfold Ce³⁺, which is apparently due to their different local geometries: one has two surface O neighbors and the other has three.

For dimer II, the four excess electrons localize on one fivefold Ce and three sixfold Ce ions. Again, the correlation between n^{Ce} and e^f exists, albeit less clearly (the PDOS in the bottom panel): e^f of the fivefold Ce is close to that of some sixfold Ce, but e^f of another sixfold Ce (denoted as Ce_{*h*} in Fig. 3) is relatively high. These features of the fivefold Ce and Ce_{*h*} can be also associated with their local geometries, most notably, a subsurface O neighbor (denoted as O_{*sub*} in Fig. 3), which itself also neighbors the two vacancies and an



(a)



(b)

FIG. 5. (Color online) (a) The electron densities of the gap states, which are localized on the eight Ce ions neighboring the vacancy tetramers (I–III) containing subsurface vacancies. For best viewing, tetramer II is shown in a periodic image. (b) The total DOSs and the Ce 4*f* partial DOSs for the surfaces containing these tetramers.

unreduced Ce⁴⁺ ion. Upon the formation of dimer II, O_{sub} exhibits a 0.65 Å upward shift (with respect to the surface plane) from its original position at the stoichiometric surface, which arises from the repulsion from its two Ce³⁺ neighbors (i.e., the fivefold Ce and Ce_h). Moreover, O_{sub} also has a 0.30 Å shift, away from the two Ce³⁺ neighbors, toward the

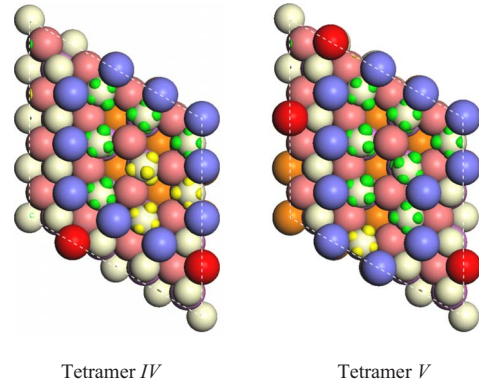


FIG. 6. (Color online) Vacancy tetramers IV and V, which can be considered as direct derivatives of SVT and contain no subsurface vacancies. The spin states are shown in green and yellow.

unreduced Ce⁴⁺ neighbor, because the Ce⁴⁺ is undercoordinated. As a result of these displacements, the distances between O_{sub} and the two Ce³⁺ neighbors are significantly larger (2.48 and 2.53 Å compared to 2.37 Å at the stoichiometric surface), suggesting that the ionic bonding between them is weakened, and consequently *e^f* of the fivefold Ce³⁺ and Ce_h appear at relatively higher energies.

We note that in the case of SV or SSV, the displacements of those O atoms adjacent to the vacancy are relatively small (generally less than 0.2 Å), compared to those in vacancy dimers. This is because in the latter, more Ce ions are reduced and larger electrostatic repulsions are generated. This result is consistent with the slightly higher *e^f* of the sixfold Ce³⁺ ion for dimers than that for monomers, which also explains why the vacancy dimers are less stable than the monomers.

C. Vacancy trimer

Taking a glance at the distribution of the spin states for SVT and DLSVC (Fig. 4), one can immediately see that the presence of the sevenfold Ce³⁺ in the latter, which has high-energy occupied *f* states, is the reason it is the less stable of the two trimers. Also analogous to the DOS for a bulk vacancy plotted in Fig. 2, the O 2*p* states for DLSVC appear at slightly higher energies than that for SVT, indicating the more weakened bonding in the former. Hence, even though the low-energy *f* states (i.e., a fourfold Ce³⁺) exist for DLSVC, the overall effect favors SVT.

The correlation between *n^{Ce}* and *e^f* is also valid for both trimers, although in the case of DLSVC, *e^f* of the fivefold Ce³⁺ are very close to those of the sixfold Ce³⁺. Other interesting details can also be found when comparing PDOS for SVT and those for dimer I or II: *e^f* of the five- and sixfold Ce³⁺ for the dimers are generally higher than those for the trimer. We ascribe this result to the fact that vacancy dimer is an exception to the general trend that VCs expose only Ce³⁺ since a fifth-layer Ce for dimer I and a second-layer Ce for dimer II, both exposed to the defect, are characteristic of Ce⁴⁺. Because the Ce⁴⁺ exposed to the defect is undercoordinated, it would pull neighboring O toward it to compensate for the loss of the ionic bonding, which would however oc-

cur at the expense of weakening other ionic bonding between Ce^{3+} and adjacent O ions, as we discussed in Sec. IV B. We should also mention that the higher energies of e^f of the five- and sixfold Ce^{3+} for dimer I or II than those for trimer SVT are consistent with the larger ΔE_v^2 calculated for the dimers than ΔE_v^3 calculated for trimer SVT (Table I).

D. Vacancy tetramer

Tetramers IV and V (Fig. 6) are more stable than tetramers I–III (Fig. 5), which is apparently due to the absence of the high e^f of the sevenfold Ce^{3+} in the former. Thus, we omit further electronic discussion for tetramers IV and V. Instead, we focus on the relative stability for the three tetramers containing subsurface vacancies (i.e., I>II or III), which could also be rationalized from the correlation between n^{Ce} and e^f of the reduced Ce ions (albeit not always evident). Due to different local geometries, some Ce^{3+} ions with same n^{Ce} may not necessarily have the same e^f and some Ce^{3+} ions with different n^{Ce} may have very similar e^f , as we have already seen in Secs. IV A–IV C.

Taking tetramers I and III [Fig. 5(a)] as examples, the Ce^{3+} ions for the former contain one sevenfold, three sixfold, three fivefold, and one fourfold ion and those for the latter contain one sevenfold, four sixfold, two fivefold, and one threefold ion. Thus, it is difficult to judge the relative stabilities based solely on n^{Ce} . However, a close examination of e^f in the PDOS [Fig. 5(b)] reveals that e^f of the threefold Ce^{3+} for tetramer III does not lie at a noticeably lower energy than that of the fourfold Ce^{3+} ion for tetramer I (as one might expect), but coincidentally at almost the same energy level; e^f of the sevenfold Ce^{3+} in tetramer III are not the same as that of the sevenfold Ce^{3+} in tetramer I (as one might expect), but somewhat higher; and e^f of the sixfold and fivefold Ce^{3+} in tetramer III are also slightly higher than those of the corresponding states in tetramer I. Clearly, these features illustrate why tetramer III is less stable than tetramer I. Furthermore, we consider that the generally higher energies of those f states for tetramer III originate from the more significant electrostatic interactions occurring for tetramer III than for tetramer I, which are evidenced by the larger geometrical changes upon the creation of the fourth vacancy in the former. For tetramer III, the newly formed threefold Ce^{3+} (originally the fourfold in DLSVC) moves 0.56 Å away from the fourth O vacancy, due to the repulsion from the two newly formed sixfold Ce^{3+} ions mediated via the O atoms in between the threefold and the sixfold ions. Meanwhile, the displacement of the threefold ion also pushes away other neighboring Ce^{3+} ions, notably, the sevenfold ion by 0.06 Å. For tetramer I, on the other hand, the repulsion, which starts between the two newly formed sixfold Ce ions and one adjacent fivefold Ce ion (originally a sixfold), is less significant: the largest displacement is for the newly formed fivefold Ce, i.e., 0.20 Å away from the two sixfold ones compared to its position before the creation of the fourth vacancy. Moreover, the displacement of the sevenfold ion is fairly small (0.02 Å) with respect to its position before the creation of the fourth vacancy.

We note from above that the larger atomic displacement always occurs to the lesser coordinated Ce. This is because a

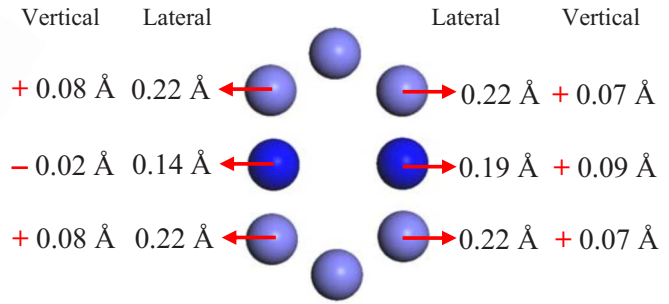
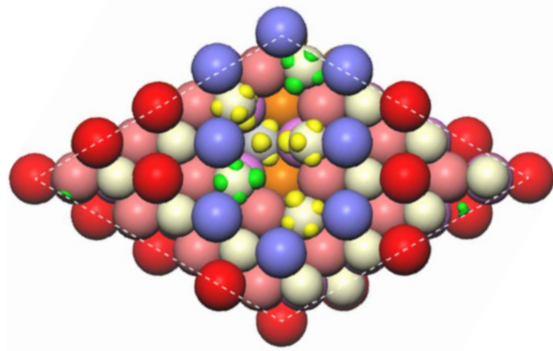
Ce with a smaller n^{Ce} is actually more charged than that with a larger n^{Ce} . Therefore, a larger electrostatic interaction between the Ce with the smaller n^{Ce} and its adjacent ions (and subsequently a larger shift of this Ce ion) is expected. We should also mention that the more charge for a Ce with a smaller n^{Ce} is mainly attributed to the more significant occupations in the $5d$ orbitals (not shown), because the Ce with the smaller n^{Ce} is closer to its neighboring O ions, allowing electron filling in these more diffused orbitals. On the other hand the occupations on the strongly localized f orbitals for reduced Ce ions with different n^{Ce} are very similar (all close to 1). The relative stability between tetramers I and II can be also understood from similar analyses to those described above, for which we do not repeat.

V. GEOMETRICAL COMPARISONS WITH EXPERIMENT AND COMMENTS ON DLSVC VERSUS SVT

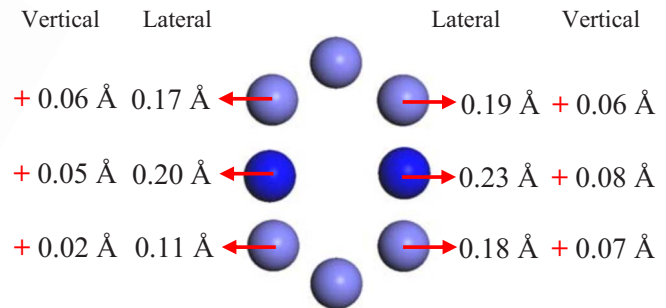
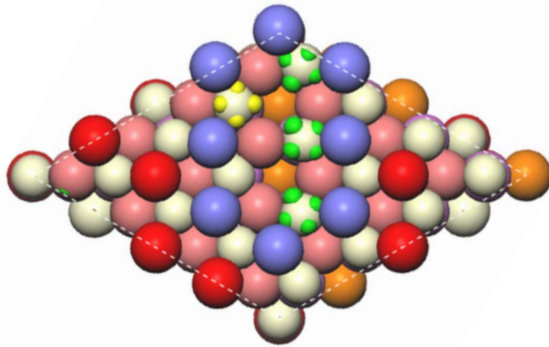
The most notable discrepancy between our calculations and some of the experiments concerns the relative stability of DLSVC versus SVT. While SVT is found to be more stable than DLSVC in this work, which is consistent with the experiments of Nörenberg and Briggs,⁷ the studies of Esch *et al.*¹¹ and Namai *et al.*⁹ suggested that DLSVC is the main defect. We should mention that our conclusion is independent of methodologies, as our tests with different U parameters and even the LDA+ U functional always favor SVT by a comfortable margin.

Esch *et al.*¹¹ showed some interesting geometries for DLSVC from their STM simulations, i.e., DLSVC is characterized by a pair of rim O atoms that face each other, one appearing ~ 0.1 Å below and one ~ 0.1 Å above the unperturbed surface. Both O atoms shift laterally toward the inside of the defect. The inward shifts are particularly interesting because one may expect that upon the creation of the VCs, the O atoms surrounding the VCs would relax outward due to the electrostatic repulsions with the reduced Ce^{3+} ions. Hence, one may ask, how well our calculation predicts the geometry of DLSVC. To illustrate this, we redraw the structure of DLSVC in Fig. 7(a), where the shifts of the six surface O atoms surrounding the VCs, with respect to their positions at the stoichiometric surface, are depicted. It becomes clear from Fig. 7(a) that upon the creation of DLSVC, all the O atoms indeed relax outward (i.e., away from the defect). However, the pair of O atoms in the middle of the irregular hexagon (highlighted in dark blue) has smaller lateral displacements than the other O atoms. As a result, these two O atoms seemingly move inward by 0.03 and 0.08 Å, respectively, with respect to the others, which is consistent with the STM image (i.e., the bright spots representing these two O atoms are closer to the defects than those representing other O atoms¹¹). The vertical shifts of these two O atoms (i.e., one moving down and one moving up) are also illustrated in Fig. 7(a). Thus, the characteristic features observed by Esch *et al.*¹¹ are well produced from our calculations.

Returning to the discrepancy, one therefore would ask why DLSVC rather than SVT is the main defect in some experiments. In the following, we propose several possible interpretations. First, although SVT is thermodynamically



(a) DLSVC



(b) Dimer II

FIG. 7. (Color online) Schematic representations of movements of the edge O atoms upon the formation of a vacancy trimer (DLSVC) and a vacancy dimer (dimer II). The lateral shifts are depicted by arrows and the vertical shifts are depicted by “+” and “-” signs, which mean moving away or toward the surface plane, respectively. The middle O pairs in the irregular hexagons are highlighted in dark blue.

more stable from our calculations, whether or not its formation is also kinetically more favorable remains an open question. We note in the literature that the different observations in STM were attributed to different sample treatments in the study of Namai *et al.*⁹ In accordance with this explanation, we speculate that during the cooling process for the STM imaging, DLSVC created at elevated temperatures may be able to maintain its integrity rather than transforming to more stable SVT due to possible kinetic barriers. This scenario is quite possible, considering that the transformation from DLSVC to SVT would involve an O diffusion into the subsurface vacancy, for which high temperatures are required.¹¹ Furthermore, we note that even the more stable trimer, SVT, is slightly less stable than the monomers (as can be seen in Table I), which suggests that SVT, like DLSVC, could also just be kinetically stable.

Second, we consider that DLSVC is quite similar to dimer II in the sense that both have two surface O vacancies and both are surrounded by six O atoms (i.e., the shape of an irregular hexagon). Although DLSVC involves a subsurface O vacancy, because of the difficulty in directly observing and

precisely locating subsurface O vacancies in STM,¹² there might be a chance that dimer II could be mistaken as DLSVC due to the resemblance of the two defects. Figure 7(b) shows the main geometrical change of the six O atoms upon the formation of dimer II, in which an interesting difference emerges when compared with DLSVC. Unlike the seemingly inward shifts of the two middle O atoms for DLSVC (relative to neighboring rim atoms), the two middle O atoms for dimer II shift outward slightly [Fig. 7(b)]. Hence, this difference would be useful to distinguish the two defects, although it might be a challenge in experiment to identify such a small displacement as a few hundredths of angstroms. Recalling the suggestion of nonobservation for dimer II,¹¹ clearly, a revisit of the possibility of dimer II in experiment would help clarify this issue.

Third, our investigations on vacancy tetramers provide further insight to the growth of LSVCS which appear to occur preferentially in a straight manner.¹¹ Let us first suppose that DLSVC has somehow already been formed on the surface, the most stable tetramer containing a subsurface vacancy must be linear (i.e., tetramer I) rather than other pos-

sible shapes (i.e., tetramers II and III), as we discussed earlier. Moreover, the formation energy for the fourth vacancy of the linear tetramer I (with respect to DLSVC) is similar to that for the single vacancy (SV or SSV) or that for the third vacancy of SVT. This indicates that if SV or SSV or SVT form under the right experimental conditions, the linear tetramer could also form in the similar circumstances provided that DLSVC is already present on the surface. It is worth mentioning that the most stable tetramer among all the possibilities would still be IV or V, which may be viewed as direct derivatives of SVT. However, the formation of these tetramers *from* DLSVC may be hindered kinetically because it would again involve an O diffusion into the subsurface vacancy, which is unlikely to occur at 300 °C (the STM imaging condition¹¹) due to the diffusion barrier presented.

Not only would the linear vacancy tetramer be expected from DLSVC, we also expect that linear vacancy pentamer, hexamer, etc. (i.e., gradually removing a further O atom at either end of the linear VCs) would likely be more stable than other possible shapes of vacancies containing subsurface vacancies. This is because the possible ways to create the $(n+1)$ th vacancy from the linear VC containing n vacancies will be similar to those described in Sec. III (i.e., releasing an O atom associated with a different Ce^{3+} ion). For the electronic reasons similar to those given in Sec. IV C, releasing a further O atom at the either end of the linear VCs would be the most favorable scenario, as it would cause the least electrostatic repulsion. Hence, the vacancy growth from DLSVCs could proceed in a linear fashion, which is exactly the case observed in the experiment of Esch *et al.*¹¹

VI. IMPLICATION IN CATALYSIS

The energy ordering of the filled f states of different Ce^{3+} ions has an interesting implication in the ceria-supported gold system, which is widely regarded as a promising catalyst for the water-gas shift reaction. From our recent study of Au adsorption at an O vacancy at the $\text{CeO}_2\{111\}$ surface,³¹ the electronic picture for the adsorption can be described as follows. Upon Au adsorption, the f electrons, which are originally localized at a Ce^{3+} , enter into the $6s(\text{Au})$ orbitals; ionic bonding develops between $\text{Au}^{\delta-}$ and adjacent Ce ions. This adsorption mechanism implies that the adsorption energetics could be closely related to the energy level of the f states of the Ce^{3+} , which would be reoxidized by the adsorbed Au. Thus, an interesting prospect of Au adsorption can be envisaged on VCs, where various f states are presented.

We calculate Au adsorption at DLSVC, in which four-, five-, six-, and sevenfold Ce^{3+} ions exist. Compared to the adsorption energy at SV (-2.29 eV), the adsorption becomes much stronger at DLSVC (the adsorption energy is -3.18 eV). The difference in the adsorption energies can be attributed to the different Ce^{3+} ions in the two cases, which are reoxidized to Ce^{4+} by the adsorbed Au: the Ce^{3+} ion is sixfold for the SV, whereas it is sevenfold for DLSVC [Fig. 8(a)]. Because the filled f states of the sevenfold Ce^{3+} are at higher energies than those of the sixfold Ce^{3+} , the elimination of the former spin states would stabilize the adsorption

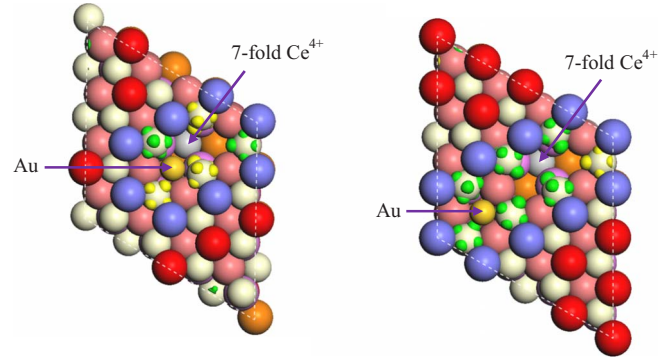


FIG. 8. (Color online) The spin states for Au adsorption at the linear vacancy trimer (DLSVC) and linear vacancy tetramer (i.e., tetramer I). In the latter case, although the Au sits at the third-nearest hollow site toward the sevenfold Ce ion, the sevenfold ion is still oxidized.

system more than it would in the latter case. We note that there are three different sites for the Au adsorption at DLSVC, namely, the three hollow sites that are surrounded by Ce^{3+} ions. However, we find that the adsorption energy is almost independent of the adsorption sites because the reoxidized Ce^{3+} is always the sevenfold one in all three adsorption cases. This feature is noted, even in situations where hollow sites do not immediately neighbor the sevenfold Ce^{3+} . Taking tetramer I as an example [Fig. 8(b)], the reoxidized Ce^{3+} is still the sevenfold one, even if Au adsorbs at the third-nearest hollow site from it. Of course, we should mention that at SVT, Au adsorption energy does not alter very much (by ~ 0.2 eV) compared to that on the single SV since in both cases the sixfold Ce^{3+} ions would be reoxidized.

The strengthened Au adsorption at VCs is interesting, considering the current controversy on the anchoring site of the Au nanoparticle on ceria, namely, whether the nanoparticle is locked into O vacancies or Ce vacancies in the ceria lattice.³⁴ This issue is often simplified to the question of which vacancy site is the most stable for Au atom adsorption.³⁵ We have shown in a recent study that a single Ce vacancy is much harder to form and much less stable than an O vacancy, and thus the Ce vacancy model may not be favored for Au adsorption.³⁶ The finding of the enhanced adsorption on VCs here would certainly add more favor to the O vacancy model. Of course, one may argue that the vacancy formation energy should also be taken into account and thus the overall adsorption energy may be different. Nevertheless, given a pre-existing VC, the adsorption on the VC would be clearly preferred.

VII. CONCLUSION

To recap, we summarize below the main conclusions that have been reached from this study:

(1) SV is as stable as SSV, which agrees with the similar coverages of the two defects observed experimentally at slightly reduced surfaces.

(2) In addition to the surface dimer containing a subsurface O suggested from experiment, the dimer of two surface O vacancies is also found to be stable.

(3) For the vacancy trimers, the linear-type (i.e., DLSVC) defect is less stable than the triangular type (i.e., SVT), mainly because of the presence of the high-energy f states of an inner sevenfold Ce ion near the former defect.

(4) Analogous to the relative stability between SVT and DLSVC, the tetramers containing no SSV are more stable than those containing SSV. In the latter cases, the tetramer with the linear shape appears to be the most stable, suggesting that the vacancy clusters could grow in a straight manner provided that DLSVC pre-exists.

(5) The main electronic change upon O removal is the electron localization on Ce ions, which plays the vital role in determining the stabilities of vacancies. A general correlation between the coordination number of Ce^{3+} and its energy for

the filled f states is identified; namely, the higher the coordination number is, the less stable the Ce^{3+} would be.

(6) The energy ordering of filled f states of Ce^{3+} has an interesting implication in ceria-supported gold systems: Au adsorption is stronger at DLSVC than at a single vacancy because the spin in the high-energy f states of the sevenfold Ce^{3+} is eliminated by the adsorbed Au.

ACKNOWLEDGMENTS

We acknowledge the Cambridge Isaac Newton Trust (C.Z.), and The Royal Society (S.J.J.). A.M. was supported by the EURYI scheme (see www.esf.org/euryi) and the EPSRC-GB.

*Author to whom correspondence should be addressed; sjj24@cam.ac.uk

¹G. A. Deluga, J. R. Salge, L. D. Schmidt, and X. E. Verykios, *Science* **303**, 993 (2004).

²S. Park, J. M. Vohs, and R. J. Gorte, *Nature (London)* **404**, 265 (2000).

³A. Trovarelli, *Catal. Rev. - Sci. Eng.* **38**, 439 (1996).

⁴R. K. Grasselli and J. D. Burrington, *Adv. Catal.* **30**, 133 (1981).

⁵Q. Fu, H. Saltsburg, and M. Flytzani-Stephanopoulos, *Science* **301**, 935 (2003).

⁶Z. Liu, S. J. Jenkins, and D. A. King, *Phys. Rev. Lett.* **94**, 196102 (2005).

⁷H. Nörenberg and G. A. D. Briggs, *Phys. Rev. Lett.* **79**, 4222 (1997).

⁸H. Nörenberg and G. A. D. Briggs, *Surf. Sci. Lett.* **424**, L352 (1999).

⁹Y. Namai, K. Fujui, and Y. Iwasawa, *J. Phys. Chem. B* **107**, 11666 (2003).

¹⁰Y. Namai, K. Fujui, and Y. Iwasawa, *Catal. Today* **85**, 79 (2003).

¹¹F. Esch, S. Fabris, L. Zhou, T. Montini, C. Africh, P. Fornasiero, G. Comelli, and R. Rosei, *Science* **309**, 752 (2005).

¹²S. Torbrügge, M. Reichling, A. Ishiyama, S. Morita, and Ó. Custance, *Phys. Rev. Lett.* **99**, 056101 (2007).

¹³C. T. Campbell and C. H. Peden, *Science* **309**, 713 (2005).

¹⁴M. Nolan, S. Grigoleit, D. C. Sayle, S. C. Parker, and G. W. Watson, *Surf. Sci.* **576**, 217 (2005).

¹⁵S. Fabris, G. Vicario, G. Balducci, S. de Gironcoli, and S. Baroni, *J. Phys. Chem. B* **109**, 22860 (2005).

¹⁶B. Herschend, M. Baudin, and K. Hermansson, *J. Chem. Phys.* **126**, 234706 (2007).

¹⁷M. V. Ganduglia-Pirovano, A. Hofmann, and J. Sauer, *Surf. Sci. Rep.* **62**, 219 (2007).

¹⁸G. Kresse and J. Hafner, *Phys. Rev. B* **49**, 14251 (1994).

¹⁹G. Kresse and J. Furthmüller, *Comput. Mater. Sci.* **6**, 15 (1996).

²⁰G. Kresse and J. Furthmüller, *Phys. Rev. B* **54**, 11169 (1996).

²¹P. E. Blöchl, *Phys. Rev. B* **50**, 17953 (1994).

²²G. Kresse and D. Joubert, *Phys. Rev. B* **59**, 1758 (1999).

²³J. P. Perdew, in *Electron Structure of Solids '91*, edited by P. Ziesche and H. Eschrig (Akademie, Berlin, 1991).

²⁴V. I. Anisimov, J. Zaanen, and O. K. Andersen, *Phys. Rev. B* **44**, 943 (1991).

²⁵A. Rohrbach, J. Hafner, and G. Kresse, *J. Phys.: Condens. Matter* **15**, 979 (2003).

²⁶G. Kresse, P. Blaha, J. L. F. Da Silva, and M. V. Ganduglia-Pirovano, *Phys. Rev. B* **72**, 237101 (2005).

²⁷C. Loschen, J. Carrasco, K. M. Neyman, and F. Illas, *Phys. Rev. B* **75**, 035115 (2007).

²⁸J. L. F. Da Silva, M. V. Ganduglia-Pirovano, J. Sauer, V. Bayer, and G. Kresse, *Phys. Rev. B* **75**, 045121 (2007).

²⁹D. A. Andersson, S. I. Simak, B. Jahansson, I. A. Abrikosov, and N. V. Skorodumova, *Phys. Rev. B* **75**, 035109 (2007).

³⁰C. W. M. Castleton, J. Kullgren, and K. Hermansson, *J. Chem. Phys.* **127**, 244704 (2007).

³¹C. Zhang, A. Michaelides, D. A. King, and S. J. Jenkins, *J. Chem. Phys.* **129**, 194708 (2008).

³²M. Nolan, S. C. Parker, and G. W. Watson, *Surf. Sci.* **595**, 223 (2005).

³³Note that we rule out the possibility of removing a subsurface O (i.e., an O associated with the sevenfold Ce^{3+}), which would lead to more reduced sevenfold ions and consequently decrease further the stability of the surface. Moreover, the resultant geometry of neighboring subsurface vacancies would not agree with the experimental pattern (Ref. 12). We also omit the discussion of removing an O (other than O_I) which is also associated with a sixfold Ce^{3+} because the resultant vacancy tetramer would have the same shape as tetramer II, and would have very similar energy and electronic structure to tetramer II too. We also rule out the possibility of removing an O (other than O_{II}) which is also associated with a fivefold Ce^{3+} . This is because the eight excess electrons, owing to the four vacancies, would localize on eight Ce ions exposed to the defect, whereas in the resultant configuration, there are only seven such Ce ions.

³⁴R. Burch, *Phys. Chem. Chem. Phys.* **8**, 5483 (2006).

³⁵D. Tibiletti, R. Amieiro-Fonseca, Y. Chen, J. M. Fisher, A. Goguet, C. Hardcare, P. Hu, and D. Thompsett, *J. Phys. Chem. B* **109**, 22553 (2005).

³⁶C. Zhang, A. Michaelides, D. A. King, and S. J. Jenkins, *J. Phys. Chem. C* (to be published).